SUPPLEMENTARY INFORMATION
DOI: 10.1038/NGEO761

Snowfall increase in coastal East Antarctica linked with southwest Western Australian drought

Tas D. van Ommen and Vin Morgan

Australian Antarctic Division and Antarctic Climate and Ecosystems Cooperative Research Centre, Private Bag 80, Hobart. 7001. Tasmania, Australia.

DOI: 10.1038/NGEO761

Southwest Western Australia: Stations and data sets

Locations of meteorological stations with high quality precipitation records are shown in Fig. S1. Rainfall data for these stations were obtained from the Bureau of Meteorology[39], along with the SWWA regional average record[40]. It should be noted that the SWWA composite from the Bureau is *not* an average of the high quality station network, but a separately derived product. The gridded data set used in Fig. 2b is produced for the Australian Water Availability Project (AWAP) and is available from the Bureau of Meteorology[41].

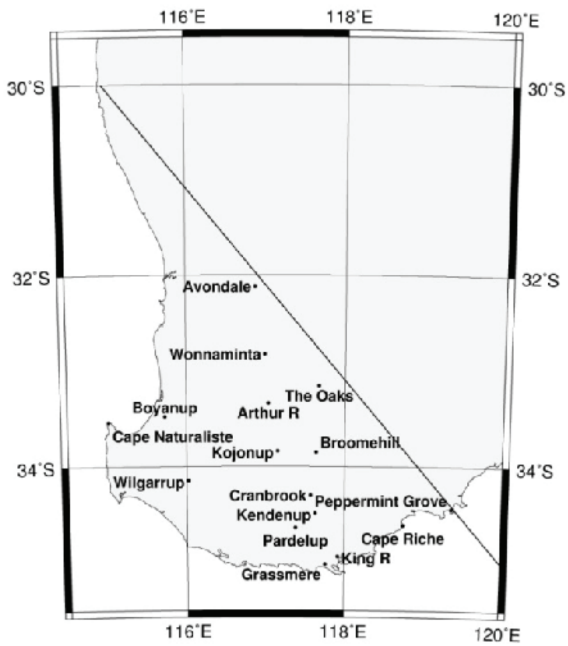

Figure S1. Map of the SWWA region with the stations for which high quality precipitation data are available. The line marks the conventional SWWA boundary, connecting 115°E,30°S to 120°E,35°S.

SWWA Station correlations with LD

Correlation values between the LD annual precipitation series and winter (June-August) precipitation are listed in Table S1 for high quality precipitation stations in SWWA. Several of these LD-SWWA correlations are comparable to inter-region correlations between SWWA precipitation values themselves: the median inter-region correlation for 5-year smoothed data, excluding the SWWA regional average, is $r_5 = 0.57$, rising to $r_5 = 0.63$ if the southern coastal stations C. Riche and Peppermint Grove are excluded.

The drought in the latter decades of the records introduces a trend in the records that accounts for a minor component of the observed correlations. For example, correlations between the detrended LD series and the detrended SWWA Avg are $r_{ann} = 0.12$ and $r_5 = 0.47$ for the annual and 5-year smoothed data respectively.

Station	ID	Lon (°E)	Lat (°S)	Start	End	r_{ann}	N^{eff}	r_5	N_5^{eff}
C. Naturaliste	9519	115.02	33.54	1904	2004	**–0.19**	100	–0.48	12
Boyanup	9503	115.73	33.48	1898	2002	**–0.22**	103	**–0.69**	9
Wilgarrup	9619	116.02	34.15	1901	2004	–0.14	101	–0.39	8
Arthur R.	10505	117.03	33.34	1891	1997	**–0.18**	107	**–0.64**	10
Kojonup	10582	117.15	33.84	1885	1996	–0.06	111	–0.37	11
Pardelup	9591	117.38	34.64	1900	1998	–0.07	99	–0.52	9
Cranbrook	10537	117.57	34.30	1891	1989	**–0.23**	98	**–0.58**	9
Kendenup	9561	117.63	34.49	1905	2004	–0.13	98	–0.47	9
Broomehill	10525	117.64	33.85	1891	2004	–0.09	114	–0.45	11
The Oaks	10636	117.67	33.16	1907	1985	–0.13	79	–0.16	11
Wonnaminta	10658	116.99	32.83	1905	2002	**–0.19**	98	–0.52	10
Avondale	10795	116.87	32.12	1908	2004	–0.10	97	–0.32	13
Grassmere	9551	117.76	35.02	1903	2002	–0.09	99	–0.36	10
King R.	9564	117.92	34.94	1904	2004	–0.09	101	–0.20	12
C. Riche	9520	118.75	34.61	1897	2004	0.02	108	0.15	13
Peppermint Gv.	9594	119.36	34.44	1904	2004	0.00	102	0.20	13
SWWA Avg	...	...	...	1900	2004	–0.16	105	**–0.55**	10

Table S1. Station details and correlation with annual LD snow accumulation for individual SWWA station winter (JJA) averages. Station ID is the Bureau of Meteorology identifier of each station. Stations listed are 'high quality precipitation records' from within the SWWA region. Correlation values are computed for the annual timeseries (r_{ann}) and for the 5-year smoothed (r_5). Bold coefficients indicate $P<0.05$ (1-tailed t-test); underlined coefficients $P<0.1$. Effective sample sizes (N^{eff} *and* N_5^{eff}) are calculated with account for autocorrelation in the timeseries (see methods).

Non-climatic noise in the LD precipitation series

In evaluating the strength of the correlation between LD and SWWA, and the significant impact of smoothing the series, we must consider the impact of various 'non-climatic' influences on the preserved snow accumulation record. As noted in the main text, several factors introduce such noise which we will consider here: lack of seasonal specificity, snow surface-relief, timing noise, evaporative loss and wind removal.

While the ice core record resolves sub-seasonal variability at Law Dome, the data lack clear subannual markers that can be tied to calendar dates, especially in the winter period. For mid-summer, studies have established that the timing of summer-peaking species, and the phasing to photochemically controlled hydrogen peroxide, give a reliable *average* timing for early- to mid-January.[35] For this reason, we only derive annual (mid-January to mid-January) averages in accumulation. Given that the signal we are most interested in corresponds to June-August SWWA precipitation, one might expect a shared variance between our annual series and a 'true' JJA series of ~25% ($r = 0.5$). In fact, from our knowledge of the site and estimates based on approximate partitioning snowfall into two seasons[42] we see overall annual variability is dominated by winter. Over ~700 years, we find that the winter 'half' of the year correlates with

 DOI: 10.1038/NGEO761

annual snowfall at $r = 0.67$ so we estimate the shorter JJA signal could correlate with measured annual accumulation with up to $r_1 \sim 0.6$.

Estimation of the impact of snow surface relief is easier, based on a number of replicate cores that cover overlapping time-periods at the LD site. We find correlations typically of $r_2 \sim 0.95$.

Timing noise due to variations in the phasing of our January marker is estimated with a simple monte-carlo method. We introduce a root-mean-square timing error of 0.1 year and find that correlation falls to $r_3 = 0.9$.

To estimate the impact of evaporative losses we used data from the polarLAPS climatology for the period 1998-2008 (N. Adams, *personal communication*) for the nearest grid point to the LD site. We find that evaporation is a small term that has correlated variability with precipitation and in fact the P-E (precipitation minus evaporation) correlates with precipitation with $r_4 = 0.99$.

Finally, wind removal is noted, but not estimated. While mean wind speed at Law Dome is not high and the site is not subject to katabatic winds, cyclonic storms are common, and indeed the main source of precipitation. Analysis of Antarctic surface mass balance indicates that wind-driven snow-loss has a substantial impact in many areas of East Antarctica.[43]

Thus combining the four terms quantified here and acknowledging the neglect of a potentially important term in the wind removal, we arrive at an estimate for the correlation between 'true' precipitation at LD and preserved accumulation of

$r = r_1.r_2.r_3.r_4 = 0.5$.

So, this is an upper limit on the expected correlation between LD and SWWA in the presence of a perfect climate teleconnection. In reality, with inclusion of weather noise and neglected effects, the observed correlations of around $r = 0.2$ appear reasonable.

If the noise sources are independent of the underlying climatological connection then the smoothing of the series over a number of years is also expected to lead to higher correlations, as is observed.

NCEP Composites for LD high and low precipitation

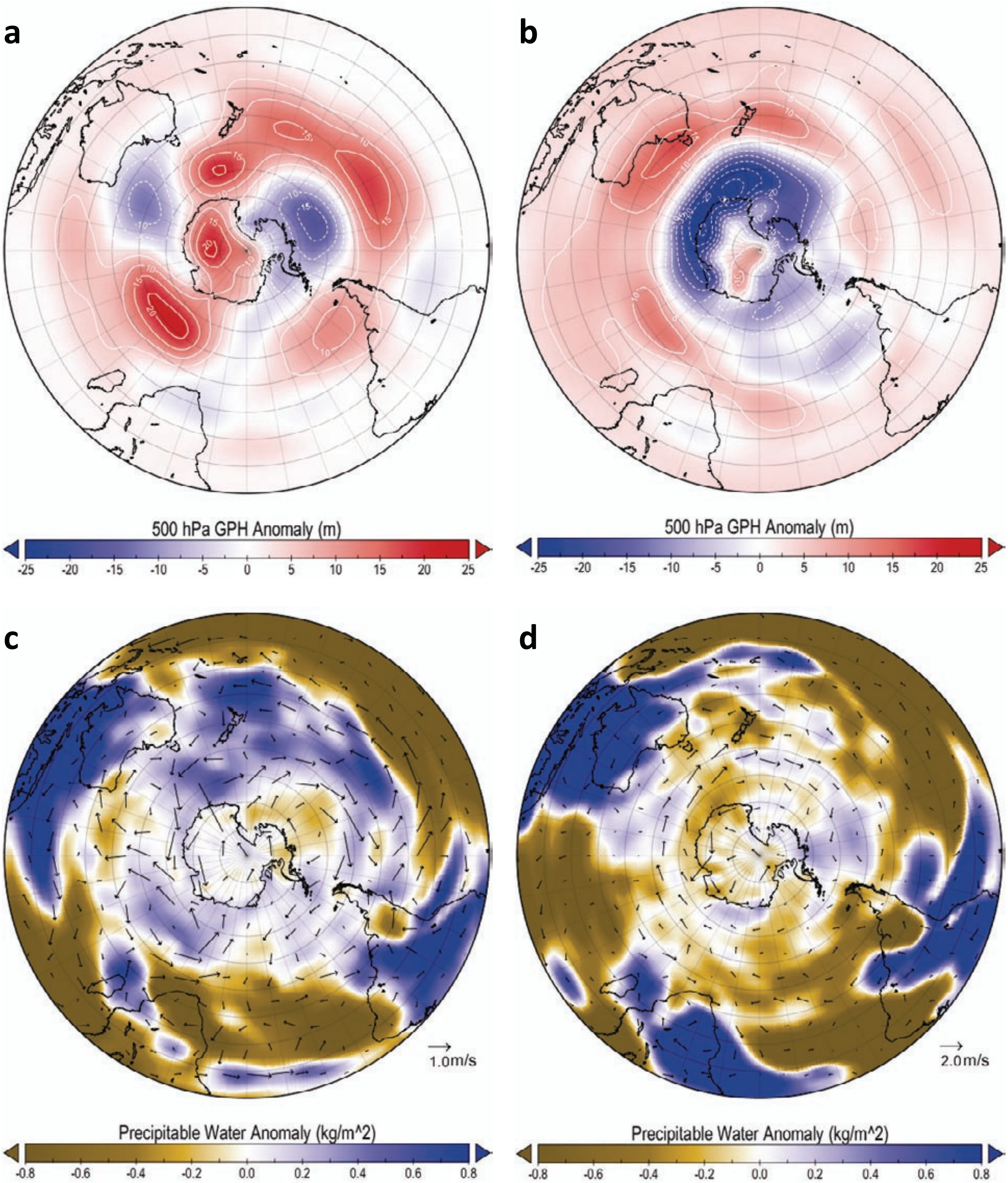

Figure S2. NCEP composite anomaly fields for high (a,c) and low (b,d) LD precipitation years over the period 1979-2004. a,b show 500 hPa geopotential height anomalies and **c,d** show the surface precipitable water anomalies with wind anomalies (500 hPa) overlaid. Note change of wind vector scale between **c** and **d**.

DOI: 10.1038/NGEO761

Composite anomalies: general observations

We computed composite NCEP anomaly fields for years with high and low LD precipitation over the period 1979-2004 (Fig. S2). The high-LD precipitation years (1980,81,84,89,96,2001) are defined as those where precipitation was in the upper quartile for the period, and are shown in the left-hand panels (Fig. S2a, S2c). The low LD precipitation years (1994,95,97,99,2000,2003), the lower quartile in precipitation, are shown in the right-hand panels. The pressure field (geopotential height for the 500 hPa surface, Fig. S2a) for high LD precipitation years (LDHi) resembles the correlation field (1979-2004) in Fig. 1 (main text), with a marked low pressure anomaly extending from southern Australia to the East Antarctic coast, with a centre near 50°S. The pressure anomalies have a predominant long-wave 3 pattern. In contrast, the low LD precipitation composite (LDLo) shows a zonal pressure pattern (Fig. S2b) with a ridge of positive anomalies extending across southern Australia from Western Australia (WA) through to New Zealand (NZ). The wind anomalies (at 500 hPa, and depicted superimposed on the precipitable water fields in the lower two panels) reflect the pressure patterns, showing circulation in the LDHi mode (Fig. S2c) bringing east to north-easterly flow to LD and the East Antarctic coast, and southerly flow to the southern tip of WA. The LDLo mode (Fig. S2d) has strengthened circumpolar westerlies around East Antarctica and north to north-easterly flow across WA and into SWWA. The precipitable water fields show the effect of the circulation in each case: in the LDHi mode, moist air extending from the north to the coast of East Antarctica and dry air extending from southwest of SWWA and inland over the region; in the LDLo mode, moist air extends from the north all the way south over SWWA, while the East Antarctic coast is marked by negative moisture anomalies.

We draw attention here to the pattern of meridional winds in Fig. S2c, associated with the anomalous precipitation in recent decades. As discussed in the main text, the northward flow south of SWWA and the southward flow onto coastal East Antarctica from NZ are both features identified in Cai and Cowan[8] as trends in forced model simulations.

We also computed correlations and anomaly maps using the ERA-40 reanalysis set, and for different tropospheric levels, and the features observed are fully consistent with those discussed here. Although we show precipitable water fields here, we also investigated the results using precipitation rate fields. The precipitation rate fields also share the salient features in both correlation (Fig. 1b) and composite anomalies (Fig. S2c, S2d) although the patterns are not as smooth and readily associated with broad circulation as is the case for precipitable water. We also had some concern that topographical influences, especially near the Antarctic coast make precipitation rate a potentially more uncertain indicator.

We note that the SLP pattern here associated with dry SWWA conditions (Fig. S2a) differs from patterns identified in a study[10] investigating synoptic scale SLP patterns and SWWA rainfall. We attribute this difference to the deliberately limited physical domain and different timescale of the variability considered. In their discussion of the self-organising map technique, the authors note that inclusion of areas eastward tended to dominate the classification. As can be seen in this study centres of action both south and east of the domain need to be included to discriminate the influence of the low pressure patterns that are embedded in predominantly zonal flow from those with meridional connection to higher latitudes.

An Australian-sector zonal wave three index

In order to explore the role of the strength of the wave three pattern in the Australian sector we have computed an index based on the pressure difference between the high centre south of NZ and the low south of SWWA. We chose two regions based on inspection of zonal anomalies of the 500 hPa geopotential height (GPH) field, and in particular the degree of correlation with LD accumulation and SWWA precipitation. The regions selected were at 110° – 115°E and 155° – 160°E , both extending from 45° – 65°S. Note these are close to the centres of the ZW3 patterns shown in Raphael's derivation of her ZW3 index.[30]

We used NCEP reanalysis data for construction of this 'Australian sector' zonal wave three index (AZ3). We note that limitations in the NCEP data set, especially prior to the satellite era (pre-1979) have been identified by various studies (see, *e.g.* discussion by Raphael[30]), and that seasonal trends in particular may be misleading for the earlier period. The index computed here is based on annual averages which should reduce any seasonal effects, but we also repeated the derivation of AZ3 using ERA-40 data instead and confirm that the results are robust.

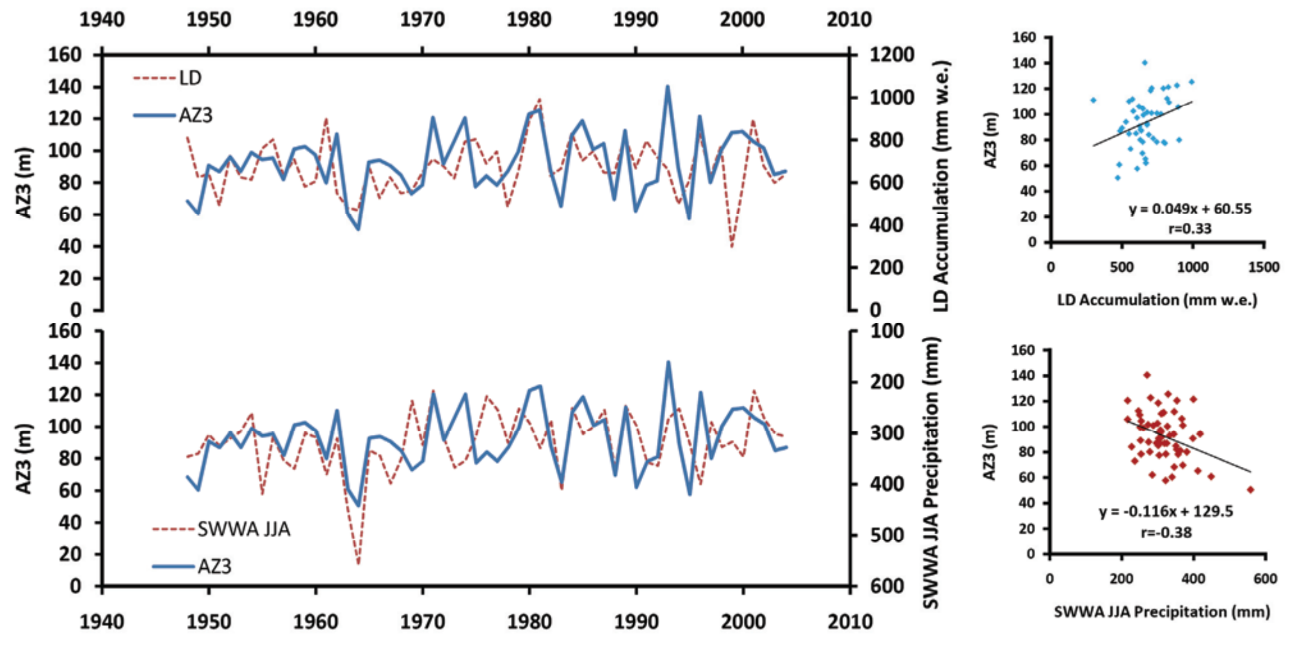

Figure S3. AZ3 index timeseries with LD and SWWA JJA precipitation series for comparison (note inverted axis for SWWA JJA). Scatter plots for the two pairs of series are shown for the period 1958-2004.

 DOI: 10.1038/NGEO761

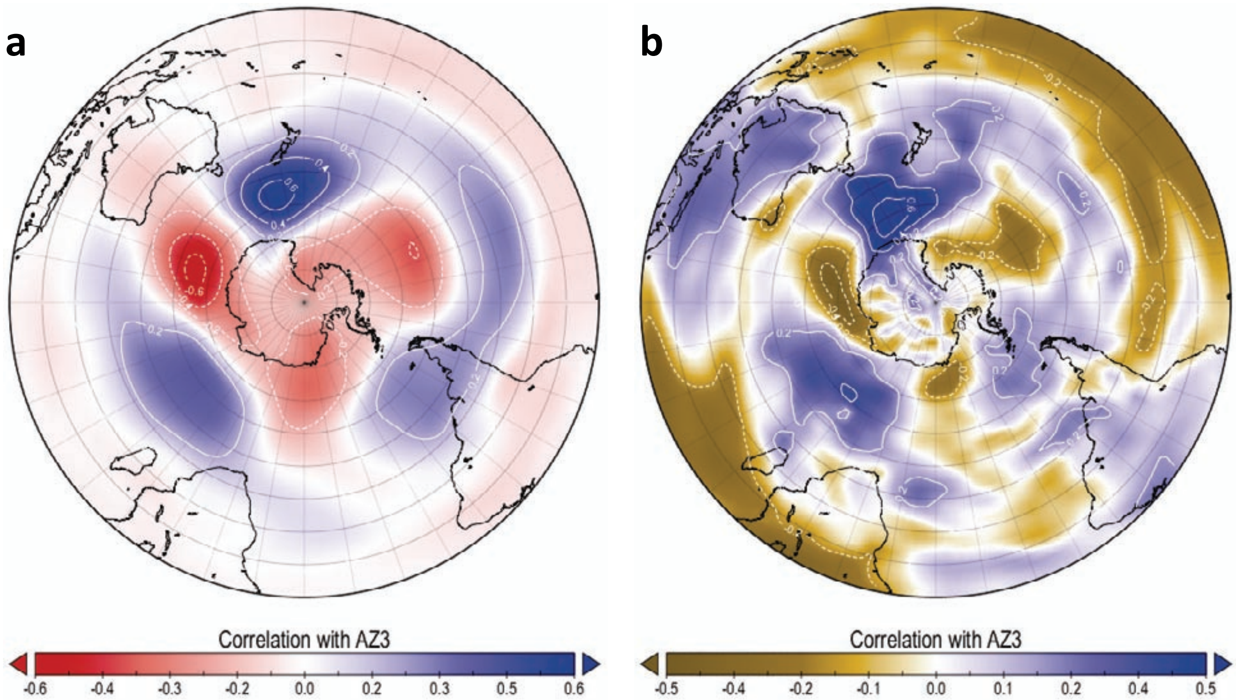

Figure S4. Correlations of AZ3 index with NCEP fields over 1958-2004. a, 500 hPa geopotential height, **b**, surface precipitable water.

AZ3 index: General observations

The AZ3 series is shown in Fig. S3 with precipitation series for LD and SWWA JJA. As noted in the main text, the correlations in each case are statistically significant (for LD, $r = 0.33$, $P = 0.01$; for SWWA, $r = -0.38$, $P = 0.004$) although the trend of 2.1% per decade is not. Repeat computation of an analog of AZ3 series using ERA-40 reanalysis shows very similar overall relationship with LD ($r = 0.41$) and SWWA ($r = -0.23$). The ERA-40 version shows minor differences to AZ3, with slightly elevated values from 1973-1987, leading to stronger and statistically significant positive trend of 4.4% per decade.

The correlation map of the AZ3 index with 500 hPa geopotential height (Fig. S4a) shows that the index, while constructed for the Australian sector is still responsive to the overall Southern Hemisphere zonal wave three mode. Correlation with surface precipitable water (Fig. S4b) shows clear positive association with the moisture stream from south of the Tasman Sea to parts of coastal East Antarctica and negative association with a meridional band from the Indian Ocean sector of Antarctica to SWWA.

Law Dome 750-Year Accumulation Statistics

We computed decadal scale anomalies for the LD precipitation series as described in the main text, and found that the largest anomaly was the most recent decadal event, which began in 1970. This event appears to belong to a population with a larger mean than the remaining 56 decadal events – we reject the null hypothesis (that it comes from the same distribution) using a 1-tailed t-test, ($P = 7\times10^{-4}$). The use of a t-test does assume a normal distribution for events. Tests for non-normality confirmed the validity of this assumption: accepting the null hypothesis (Kolmogorov-Smirnov, $P = 0.28$, Lilliefors, $P = 0.88$). Also, inspection of a quantile-quantile plot supports the assumption of normally distributed data.

Relaxing this assumption and testing whether the post 1970 event is from the same distribution using a more conservative non-parametric Wilcoxon rank-sum statistic still indicates a statistically significant difference between the post 1970 event and the others ($P = 0.04$).

The 56 anomalies in the period 1250-1969 have a mean precipitation of –0.0188 m and standard deviation, 0.719 m (ice-equivalent, *i.e.* for glacial ice density 917 $kg.m^{-3}$). The post 1970 anomaly is 2.42 m (*i.e.*), which is extremely improbable from the distribution of 1250-1969 anomalies ($P = 3.4\times10^{-4}$, normal z-score).

We also recalculate the anomalies using a composite 'stack' of the available ice cores that excludes the DSS97 core (Methods). We believe that this record provides an underestimate of recent accumulation, however this series leads to the same conclusion regarding the post 1970 anomaly (albeit with lower significance).

For this alternate series, the assumption of normally distributed pre-1970 anomalies is supported with rejection of the hypothesis of a non-normal data, as above ($P<0.01$). For the pre-1970 anomalies, the mean precipitation is –0.011 m (*i.e.*) with a standard deviation 0.708 m (*i.e.*). The post-1970 anomaly has a magnitude of 1.98 m (*i.e.*), and is also highly improbable for the pre-1970 distribution ($P = 2.4\times10^{-3}$, normal z-score).

Using these probabilities, and given the mean duration of individual decadal scale anomalies (12.8 years), the post 1970 event might be expected almost once in ~38,000 years (for the preferred composite stack) or once in 5,400 years (for the alternate stack). In either case the event is clearly outside the envelope of natural variability.

Supplementary References

39. ftp://ftp.bom.gov.au/anon/home/ncc/www/change/HQmonthlyR/

40. http://www.bom.gov.au/cgi-bin/silo/reg/cli_chg/timeseries.cgi

41. http://www.bom.gov.au/jsp/awap/rain/index.jsp

42. van Ommen, T., Morgan, V. & Curran, M. A new sub-annually resolved accumulation series from Law Dome, in Earth: Our Changing Planet. Proceedings of IUGG XXIV General Assembly Perugia, Italy. JMS026-1487 (2007).

DOI: 10.1038/NGEO761

43. Frezzotti M. *et al.* New estimations of precipitation and surface sublimation in East Antarctica from snow accumulation measurements. *Clim. Dynamics*, **23**, 801-813, doi:10.1007/s00382-004-0462-5 (2004).